ENHANCING MICRO-OVEN POWER AND STIFFNESS IN ENCAPSULATED DEVICES FOR TIMING REFERENCE APPLICATIONS

Lizmarie Comenencia Ortiz[1], Dustin D. Gerrard[1], Ian B. Flader[1], Gabrielle D. Vukasin[1], David B. Heinz[1], Janna Rodriguez[1], Saisneha Koppaka[1], Dongsuk D. Shin[1], Hyun-Keun Kwon[1], Saurabh Chandorkar[2], and Thomas W. Kenny[1]*

[1]Stanford University, Stanford, California, USA

[2]IISc Bangalore, Bangalore, India

ABSTRACT

In this paper, we investigate the tradeoff between power-usage and stiffness to find an in-chip device layer micro-oven design with optimal yield. A variety of micro-ovenized double-ended tuning forks (DETFs) anchored via a serpentine heater or micro-oven are fabricated in an ultra-clean vacuum seal encapsulation process. The micro-ovens contain beams of varying lengths, widths, and thicknesses. We compare the power required to raise the micro-ovens to a fixed temperature and the yield of the devices. These results are the first report of yield statistics for in-chip device-layer ovenized devices. We show that a serpentine micro-oven located in the device layer of an encapsulated device with a thermal conductance of 0.17 mW/°C and a 25% yield, has 4X improvement over the power required for earlier, stiffer micro-oven designs.

INTRODUCTION

MEMS timing references are replacing quartz clocks in industrial applications due to their improved stability, small size, and low cost [1]. To achieve the high frequency stability required for MEMS sensors in industrial applications, temperature compensation methods are essential. Previous work has shown that a combination of passive and active temperature compensation methods can achieve the frequency stability required in timing reference applications [1-11]. Active temperature compensation can be achieved using a resistor or micro-oven embedded within the device layer, which heats only the suspended resonating element that is thermally isolated within the die [1,3-5]. This "in-chip ovenization" enables a significant size and power reduction that can heat the resonating element to a specific temperature and allow its frequency to remain constant with drastic changes in the temperature of its surroundings. Although power is significantly reduced in the device layer micro-ovenization in comparison to a cap layer micro-oven (3mW/°C) [2], the stiffness of the mechanical support may be sacrificed.

Thermal conductance depends on the length, width, and thickness of the micro-oven beams. Generally, operating power can be reduced by increasing the length of the beams and decreasing the width and thickness of the beams. As these parameters are changed to increase thermal resistance, the micro-oven becomes more flexible and therefore more prone to fatal in-process stiction, which occurs during the fabrication process [12].

It is necessary to investigate the relationship between the micro-oven stiffness and thermal conductance to determine the limits of the thermal properties that can be achieved with a micro-oven embedded in the device layer in our encapsulation process. In this paper, we study a series of devices with different micro-oven designs to find this relationship and find the tradeoff between micro-oven power and yield.

DESIGN AND FABRICATION

We study the properties of a set of micro-ovens attached at the anchor of a double-ended tuning fork (DETF), as shown in Figure 1. We model the eigenfrequency mode for the DETF inplane bending mode using the COMSOL Structural Mechanics module. The frequency of the bending mode is 1MHz at room temperature, as shown in Figure 1.

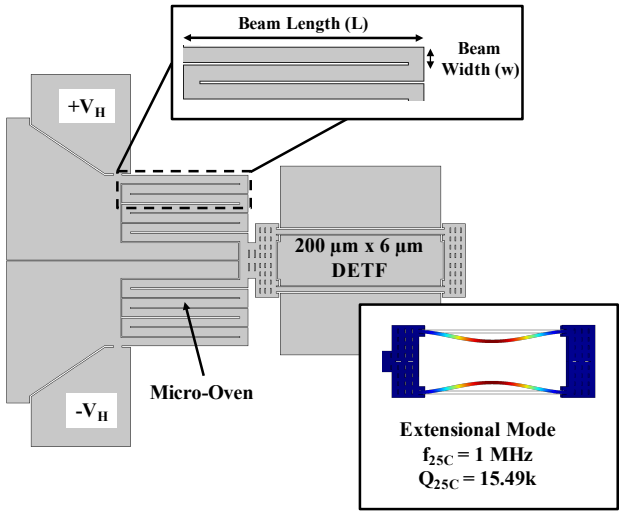

Figure 1: Diagram of micro-ovenized DETF with parameters studied.

We model the thermal conductance of the micro-oven with the COMSOL Joule Heating and Thermal Expansion module. We apply a split heater voltage of 1V at the micro-oven terminals ($+V_H$ and $-V_H$) and set the temperature at the terminals to 25°C, as shown in Figure 3. The voltage applied to the micro-oven induces an electric potential across the micro-oven beams, which elevates their temperature to approximately 100°C. The DETF structure is heated via conduction from the micro-oven. The parameters used in the simulations are defined in Table 1.

We designed and fabricated a range of micro-ovens with varying beam widths, lengths, and thicknesses to compare the thermal conductance of micro-ovens with varying stiffness. Additionally, we designed and fabricated micro-ovens with geometric variations to compare the effect of differences in the beam geometry. The variations include serpentine heaters with beam holes, round edges, and variable beam widths, as shown in Figure 2. These structures contain two suspension structures, aligned with the X and Y axis to isolate the thermal gradients in these axes, such as the ones described in [3].

We model the effective stiffness of each device using the COMSOL Solid Mechanics module. We apply a 100mN force at the tip of the DETF along the Y-axis and measured the inplane deformation of the device along the Y-axis, we similarly model the out-of-plane stiffness (Z-axis) of each device. The parameters for beam variations and simulation results are summarized in Table 2.

The devices were fabricated on p-type SOI wafers with a 40µm and a 60µm device layer using an epitaxial vacuum encapsulation

978-1-940470-03-0/HH2018/$25©2018TRF
DOI 10.31438/trf.hh2018.59

process. Each device has the same DETF resonating structure and variations in the micro-oven structure attached at the anchor. The structures had an overetch of approximately 300nm, which was accounted for in our simulations.

Table 1: Key parameters used in Joule heating and solid mechanics models.

Parameter	*Value*	*Source*
Thermal Conductivity	110.5 W/m-K	Calculated using [18]
Heat Capacity	711 J/kg-K	Estimated [10]
Electrical Conductivity	1.18E4 S/m	Wafer doping
Young's Modulus	169 GPa	[17]
Poisson's Ratio	0.064	[17]

Table 2: Summary of properties and simulation results for range of micro-ovens fabricated and tested with different dimensions.

μOven	*L (μm)*	*w (μm)*	*t (μm)*	*Effective Stiffness (N/m)*		*Thermal Resistance (mW/°C)*
				k_Y	k_Z	
1	30	5	60	21.6	96.4	0.54
2	60	5	60	4.32	86.6	0.22
3	60	10	60	50.6	199	0.62
4	90	10	60	105.9	143.2	0.41
5	150	10	60	6.58	36.8	0.19
6	120	10	40	9.36	14.4	0.20
7	150	10	40	4.38	7.84	0.13 (No yield)

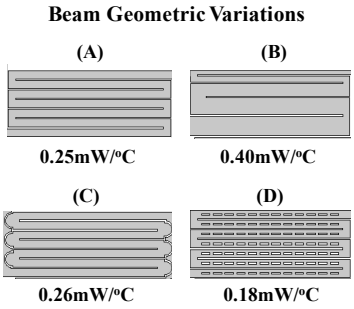

Figure 2: Summary of micro-ovens fabricated with varying geometries: (A) normal, (B) variable beam width, (C) round edges, (D) beam with holes.

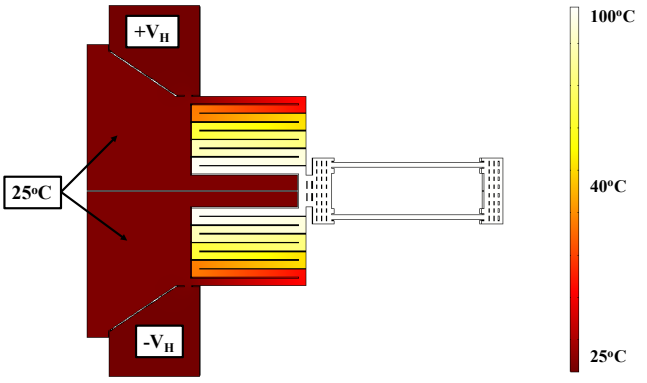

Figure 3: Temperature profile of micro-ovenized DETF with 1V applied at the micro-oven terminals and initial temperature at 25°C.

METHODS

The temperature dependence of the resonant frequency and quality factor for the bending mode of the DETF were measured from -10°C to 70°C, as shown in Figure 4. The quality factor was determined using the 3dB method of the frequency sweeps at stabilized temperatures. The frequency vs. temperature slope was -21.3ppm/°C. This ratio was used to estimate the temperature of the resonator at different heating voltages during operation of the micro-oven.

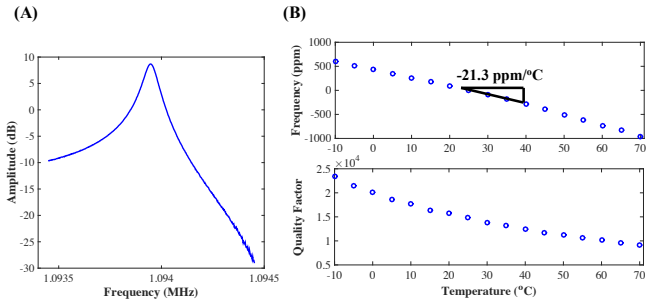

Figure 4: Characterization of DETF TCf and TCQ: (A) resonant frequency at 25°C, (B) frequency and quality factor dependence over temperature.

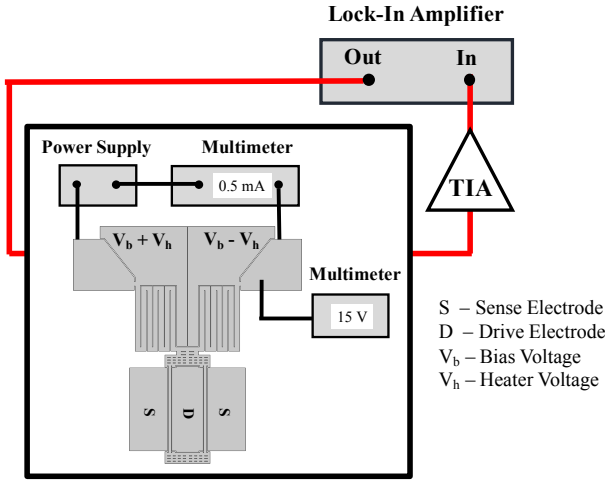

Figure 5: Experimental set up: a lock-in amplifier was used to collect open loop sweeps of the frequency over temperature.

A Zurich Instruments lock-in amplifier and transimpedance amplifiers were used in the configuration shown in Figure 5 to collect open loop frequency sweeps and measure the resonant frequency of each DETF as a function of applied micro-oven power to characterize the performance of each type of micro-oven. Split-heater voltages of 0V to 1V were applied at the terminals of each micro-oven stepwise to induce Joule heating through the beams and increase the temperature of the DETF structure. A benchtop multimeter (HP 34401A) was used to record the current and voltage through the micro-oven at each step. The ambient temperature surrounding the encapsulated die was maintained at 25°C using a benchtop temperature chamber, while the DETF temperature was elevated from 25°C to 100°C. The 75°C increase in temperature caused a change in the DETF resonant frequency of approximately 1600 ppm.

To further understand the relationship between the thermal conductance and the stiffness, we measured the survival rate of dozens of devices fabricated in the same process. We probed the devices for electrical conductivity after fabrication to determine if any two surfaces were fused into contact, or stiction occurred. We used a benchtop multimeter (HP 34401A) to measure the resistance between the surfaces.

RESULTS

Micro-Oven Power

We first characterize the performance of each micro-oven with the current and voltage relationship, shown in Figure 6. The darker lines show the low power micro-ovens, that have a steep slope versus other designs that require more power. The results in Figure 7 show that the power required to reach a device temperature of 100°C varies with the stiffness and topology of the micro-oven. The change in frequency of each DETF varies linearly with the micro-oven power. Each device had a different slope, depending on the properties of the micro-oven attached at the anchor. From these results, we find that a micro-oven with a stiffness of 15.6N/m can achieve a temperature rise of 75°C with a micro-oven power as low as 12.5mW, which is an 18X improvement over the cap layer heater architecture [2].

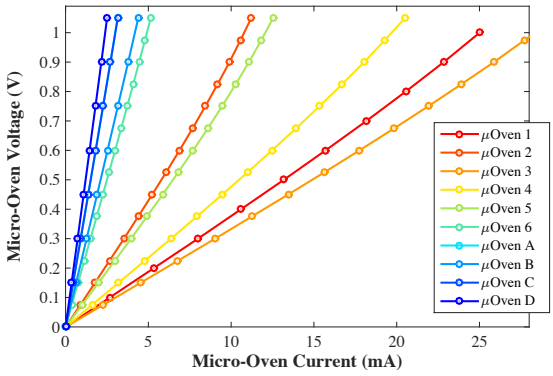

Figure 6: Current and voltage relationship for heaters tested.

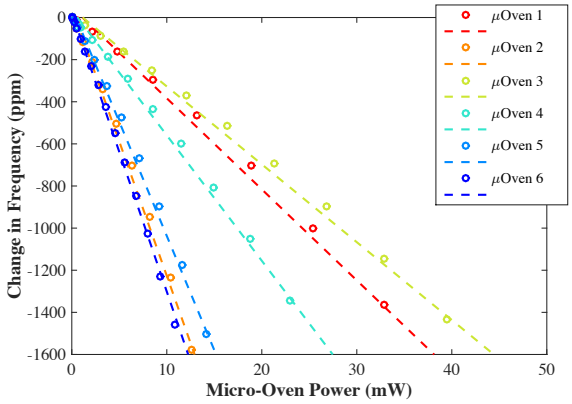

Figure 7: Change in frequency with the application of 1V at the terminals of a range of micro-ovens with varying stiffness.

Micro-Oven Geometric Variations

We compared the heating properties of micro-ovens with geometric variations on the beams, described in Figure 2. We find that modifying the geometry with round edges does not affect significantly the thermal resistance, as shown in Figure 8, since any sharp edges in the structure become smooth due to the thermal annealing step in our fabrication process; whereas adding holes to the beams increases the electrical and thermal resistance of the heater and reduces the required micro-oven power by 30%. Adding a variable beam width increases the stiffness of the beams and decreases the thermal resistance of the heater and therefore increases the power required to elevate the device temperature to 100°C.

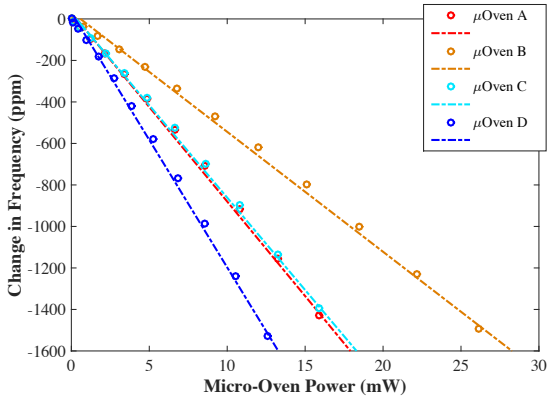

Figure 8: Change in frequency with the application of 1V at the terminals of a range of micro-ovens with varying geometry.

Micro-Oven Stiffness and Power Relation

We have explored the relationship between the micro-oven stiffness and the power required to elevate the device temperature from 25°C to 100°C. The results shown in Figure 9, demonstrate that as the effective out-of-plane stiffness of the micro-oven increases, the power increases linearly. The parameters necessary to reduce the effective stiffness of the micro-oven allow for the micro-oven to be thinner and longer, which is also necessary to reduce the power requirements. The results show that an optimal out-of-plane stiffness of 86.6N/m and a low power of 15mW can be achieved with shorter and thinner beams (L = 60μm, w = 5μm, t = 60μm).

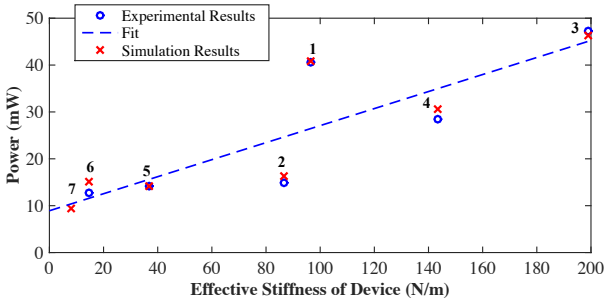

Figure 9: Power required to elevate the DETF temperature to 100°C with varying device out-of-plane stiffness (micro-ovens 1-7).

Micro-Oven Survival Rate

We demonstrate that more power-efficient ovenized devices can be designed by increasing the resistance of serpentine beams. This comes at the cost of making the device less stiff, resulting in lower yield. Our results show that an increase in the effective inplane and out-of-plane stiffness of the device increases the chances of survival by reducing the potential for fatal stiction. Stiffness and survival rate are exponentially related, as shown in Figure 10. These results show a trend of stiffer designs that require more power have less stiction. Devices with an inplane stiffness of 20-40N/m and an out-of-plane stiffness of 50-80N/m require low power and have a chance of survival of 60-80%, which makes this range suitable for our studies of timing references. Additionally, the results in Figure 10 suggest that the inplane stiffness is related to the yield of the micro-ovens with beam geometric variations (designs A-D). The double suspension structure in the X and Y axes lowers the inplane stiffness for these devices making them more prone to inplane stiction than to out-of-plane stiction.

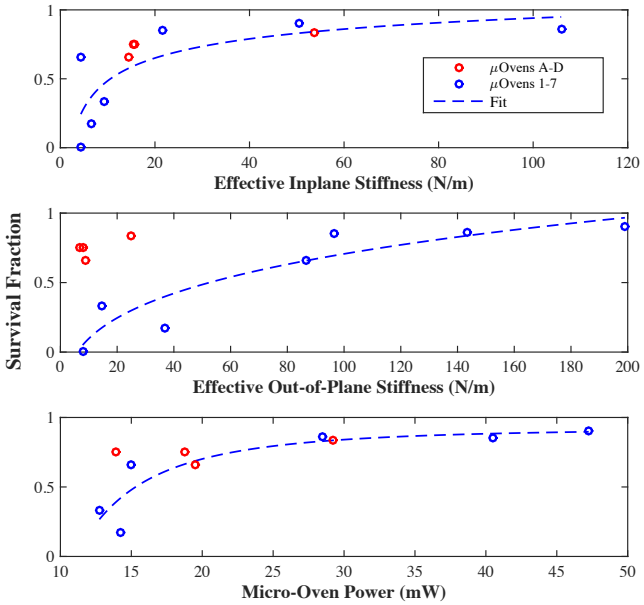

Figure 10: Survival rate of micro-ovens after fabrication with varying stiffness and power; Dozens of samples were tested.

CONCLUSION

In this paper, we investigate the relationship between micro-oven power and the yield of the device. We find that the effective stiffness of the device and the power of the micro-oven are related linearly, and that the yield of the device is related exponentially to its stiffness. Thus, there is a trade-off between in-process survival and performance of the micro-oven. We find that to minimize power and maximize the yield, we must design a micro-oven with an inplane stiffness of 20-50N/m and an out-of-plane stiffness of 50-80N/m. These results provide useful insight into micro-oven shape and variations that require low power to be used in future designs.

ACKNOWLEDGEMENTS

This work was supported by the Defense Advanced Research Projects Agency (DARPA) Precision Navigation and Timing program (PNT) managed by Drs. Robert Lutwak and Ron Polcawich under contract # N66001-12-1-4260. The fabrication work was performed at the Stanford Nanofabrication Facility (SNF), which was supported by National Science Foundation through the National Nanotechnology Infrastructure Network under Grant ECS-9731293. The author would also like to thank the National Science Foundation and the Graduate Research Program (NSF-GRFP) program.

REFERENCES

[1] C. T.-C. Nguyen, and R. T. Howe, "Microresonator frequency control and stabilization using an integrated micro oven", in Technical Digest of the 1993 Transducers Conference, Yokohama, Japan, 6/7-10/93, IEEE, (1993), pp. 1040-1043.

[2] Y. Chen, E. J. Ng, D. D. Shin, C. H. Ahn, Y. Yang, I.B. Flader, V. A. Hong, and T. W. Kenny, "Ovenized Dual-Mode Clock (ODMC) Based on Highly Doped Single Crystal Silicon Resonators", Technical Digest of the 2016 MEMS Shanghai, China, 6/24-28/16, IEEE and IEEE Robotics and Automation Soc. (2016), pp. 91-94.

[3] J. Salvia, R. Melamud, S. A. Chandorkar, S. F. Lord, and T.W. Kenny, "Real-Time Temperature Compensation of MEMS Oscillators Using an Integrated Micro-Oven and a Phase-Locked Loop," Microelectromechanical Systems,19, 1, (2010).

[4] C. Jha, M. A. Hopcroft, S. A. Chandorkar, J. C. Salvia, M. Agarwal, R. N. Candler, R. Melamud, B. Kim, and T. W. Kenny, "Thermal Isolation of Encapsulated MEMS Resonators," Microelectromechanical Systems, 17, 1, (2008).

[5] W. You, B. Pei, K. Sun, L. Zhang, H. Yang, and X. Li, "Oven controlled N++ [1 0 0] length-extensional mode silicon resonator with frequency stability of 1 ppm over industrial temperature range". Micromech. and Microeng., 27, 9, (2017).

[6] C. Y. Liu, M. H. Li, H. G. Ranjith and S. S. Li, "A 1 MHz 4 ppm CMOS-MEMS oscillator with built-in self-test and sub-mW ovenization power," Technical Digest of 2016 Int. Electron Devices Meeting, San Francisco, CA, 12/3-7/16, IEEE, (2016), pp. 26.7.1-26.7.4.

[7] L. Comenencia Ortiz, et. al, "Thermal Effects of Ovenized Clocks on Episeal Encapsulated Inertial Measurement Units", Technical Digest 2018 MEMS, Belfast, Ireland, 6/21-25/18, IEEE and IEEE Robotics and Automation, (2018).

[8] Z. Wu and M. Rais-Zadeh, "A Temperature-Stable Piezoelectric MEMS Oscillator Using a CMOS PLL Circuit for Temperature Sensing and Oven Control," Microelectromechanical Systems, 24, 6, (2015).

[9] S. Zaliasl *et al*., "A 3 ppm 1.5 × 0.8 mm 2 1.0 μA 32.768 kHz MEMS-Based Oscillator," Solid-State Circuits, 50, 1, (2015).

[10] E. Ng, V. A. Hong, Y. Yang, C. H. Ahn, C. L. M. Everhart, and T. W. Kenny, "Temperature Dependence of the Elastic Constants of Doped Silicon", Microelectromechanical Systems, 24, 3, (2015).

[11] R. Melamud, S. A. Chandorkar, B. Kim, H. K. Lee, J. C. Salvia, G. Bahl, M. A. Hopcroft, and T. W. Kenny, "Temperature-Insensitive Composite Micromechanical Resonators", Microelectromechanical Systems, 18, 6, (2009).

[12] D. B. Heinz, V. A. Hong, C. H. Ahn, E. J. Ng, Y. Yang, and T. W. Kenny, "Experimental Investigation Into Stiction Forces and Dynamic Mechanical Anti- Stiction Solutions in Ultra-Clean Encapsulated MEMS Devices," Microelectromechanical Systems, 25, 3, (2016).

[13] M. H. Li, C.-Y- Chen, C.-S. Li, C.-H. Chin, S.-S Li, "A Monolithic CMOS-MEMS Oscillator Based on an Ultra-Low -Power Ovenized Micromechanical Resonator", Microelectromechanical Systems, 24, 2, (2015).

[14] D. Yang, J.-K. Woo, S. Lee, J. Mitchell, A. D. Challoner, and K. Najafi, "A Micro Oven-Control System for Inertial Sensors", Microelectromechanical Systems, 26, 3, (2017).

[15] K. E. Wojciechowski, M. S. Baker, P. J. Clews, and R. H. Olsson, "A Fully Integrated Oven Controlled Microelectromechanical Oscillator Part I: Design and Fabrication," Microelectromechanical Systems, 24, 6, (2015).

[16] K. E. Wojciechowski, and R. H. Olsson, "A Fully Integrated Oven Controlled Microelectromechanical Oscillator Part II: Characterization and Measurement," Microelectromechanical Systems, 24, 6, (2015).

[17] M. A. Hopcroft, W. D. Nix, and T. W. Kenny, "What is the Young's modulus of silicon?", Microelectromechanical Systems, 19, 2, (2010).

[18] M. Asheghi, K. Kurabayashi, R. Kasnavi, and K. E. Goodson, "Thermal conduction in doped single-crystal silicon films." Applied Physics, 91, 8, (2002).

CONTACT

*L. Comenencia Ortiz, tel: +1-787-608-9044;
lcomenen@stanford.edu